AD-773 323

INTERPRETATION OF STRONG-MOTION EARTHQUAKE ACCELEROGRAMS USING A MOVING DISLOCATION MODEL

Lawrence S. Turnbull, Jr., et al

Texas Instruments, Incorporated

Prepared for:

Air Force Office of Scientific Research

15 November 1973

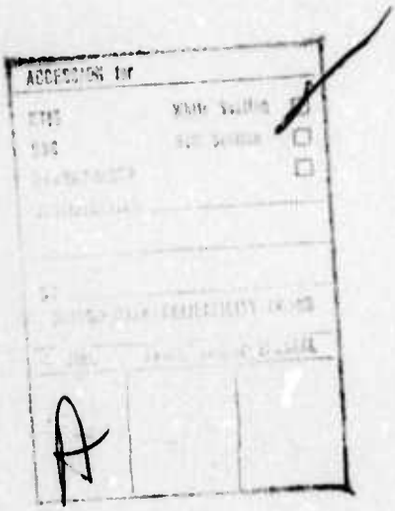

AIR FORCE OFFICE OF SCIENTIFIC RESEARCH (AFSC)
NOTICE OF TRANSMITTAL TO DDC
This technical report has been reviewed and is approved for public release IAW AFR 190-12 (7b).
Distribution is unlimited.

D. W. TAYLOR
Technical Information Officer

UNCLASSIFIED
Security Classification

AD773323

DOCUMENT CONTROL DATA - R & D
(Security classification of title, body of abstract and indexing annotation must be entered when the overall report is classified)

1. ORIGINATING ACTIVITY (Corporate author)
Texas Instruments Incorporated
Equipment Group
Dallas, Texas 75222

2a. REPORT SECURITY CLASSIFICATION
UNCLASSIFIED

2b. GROUP

3. REPORT TITLE
Interpretation of Strong-Motion Earthquake Accelerograms Using A Moving Dislocation Model

4. DESCRIPTIVE NOTES (Type of report and inclusive dates)
Semi-Annual Technical Report No. 3, 1 May 1973 - 30 October 1973

5. AUTHOR(S) (First name, middle initial, last name)
Lawrence S. Turnbull, Jr. and James C. Battis

6. REPORT DATE
15 November 1973

7a. TOTAL NO. OF PAGES
49

7b. NO OF REFS
9

8a. CONTRACT OR GRANT NO
Contract No. F44620-72-C-0073

b. PROJECT NO.
ARPA Program Code
No. 2F10

c.

d.

9a. ORIGINATOR'S REPORT NUMBER(S)
ALEX(02)-TR-73-03

9b. OTHER REPORT NO(S) (Any other numbers that may be assigned this report)
AFOSR - TR - 74 - 0022

10. DISTRIBUTION STATEMENT

11. SUPPLEMENTARY NOTES
ARPA Order No. 2134

12. SPONSORING MILITARY ACTIVITY
Advanced Research Projects Agency
Nuclear Monitoring Research Office
Arlington, Virginia 22209

13. ABSTRACT

Near-field strong-motion accelerograms of the San Fernando earthquake and three of its aftershocks recorded at Pacoima Dam were analyzed using Haskell's moving dislocation model. For the main shock, it was found that: (1) The effect of stick-slip (segmented rupture velocities) is not prominent within a moderate range of rupture velocities; (2) A hinged fault surface can produce the necessary initial negative polarity of the vertical velocity trace; (3) Using Jungles' and Frazier's (1973) solution, the Haskell model produces very large amplitudes compared to those observed. For three aftershocks (events 4, 11, 30, according to Trifunac, 1972) which occurred within six minutes of the main shock, it was found that: (1) Their solutions were characterized by small fault area (~1km^2), moderate rupture velocities (~3 km/sec), and very short rise times (~0.03 sec); (2) The dislocation particle velocities of events 4 and 30 compare with that of the main shock, but the velocity of event 11 seems too high. Without independent estimates of some of the source parameters (location, fault orientation, fault length), as with the aftershocks, the solution becomes less credible.

1/2

DD FORM 1 NOV 68 1473

UNCLASSIFIED
Security Classification

51

14. KEY WORDS	LINK A		LINK B		LINK C	
	ROLE	WT	ROLE	WT	ROLE	WT
Near-Field Earthquake Strong-Motion Records						
Dislocation Modeling of Near-Field Motion						
Stick-Slip						
Non-Planar Fault Surface						

1c

INTERPRETATION OF STRONG-MOTION EARTHQUAKE ACCELEROGRAMS USING A MOVING DISLOCATION MODEL

SEMI-ANNUAL TECHNICAL REPORT NO. 3
1 MAY 1973 TO 31 OCTOBER 1973

Prepared by
Lawrence S. Turnbull, Jr., and James C. Battis

TEXAS INSTRUMENTS INCORPORATED
Equipment Group
Post Office Box 6015
Dallas, Texas 75222

Contract No. F44620-72-C-0073
Amount of Contract: $98,994
Beginning 1 May 1972
Ending 30 April 1974

Prepared for

AIR FORCE OFFICE OF SCIENTIFIC RESEARCH

Sponsored by

ADVANCED RESEARCH PROJECTS AGENCY
Nuclear Monitoring Research Office
ARPA Program Code No. 2F10
ARPA Order No. 2134

15 November 1973

Acknowledgment: This research was supported by the Advanced Research Projects Agency, Nuclear Monitoring Research Office, under Project VELA-UNIFORM, and accomplished under the direction of the Air Force Office of Scientific Research under Contract No. F44620-72-C-0073.

//

ABSTRACT

Near-field strong-motion accelerograms of the San Fernando earthquake and three of its aftershocks recorded at Pacoima Dam were analyzed using Haskell's moving dislocation model. For the main shock, it was found that: (1) The effect of stick-slip (segmented rupture velocities) is not prominent within a moderate range of rupture velocities; (2) A hinged fault surface can produce the necessary initial negative polarity of the vertical velocity trace; (3) Using Jungles' and Frazier's (1973) solution, the Haskell model produces very large amplitudes compared to those observed. For three aftershocks (events 4, 11, 30, according to Trifunac, 1972) which occurred within six minutes of the main shock, it was found that: (1) Their solutions were characterized by small fault area (~1 km^2), moderate rupture velocities (~3 km/sec), and very short rise times (~0.03 sec); (2) The dislocation particle velocities of events 4 and 30 compare with that of the main shock, but the velocity of event 11 seems too high. Without independent estimates of some of the source parameters (location, fault orientation, fault length), as with the aftershocks, the solution becomes less credible.

TABLE OF CONTENTS

LIST OF FIGURES

LIST OF FIGURES
(continued)

LIST OF FIGURES
(continued)

LIST OF TABLES

SECTION I
INTRODUCTION

This report discusses the continuation of the work begun by Tsai and Patton (1972 and 1973) on the application of Haskell's moving dislocation model for interpreting near-field strong-motion earthquake records. We have restricted our analysis to those records obtained very close to the event, so that the whole space formulation of Haskell's model is quite reasonable.

In Section II, a review of Haskell's model is given, and a general discussion of the effect each parameter has on the theoretical waveform is presented. In particular, the effect of dip angle, rupture velocity, and total dislocation is shown by two fault plane configurations for the San Fernando main shock. The first representation uses the model of Jungles and Frazier (1973) in an attempt to fit the record at Pacoima Dam. The second representation is a somewhat simplified version of the first, but includes a segmented fault plane with variable rupture velocity, dislocation, and dip angle.

Further earthquake activity very close to the San Fernando earthquake fault plane is examined in Section III. Three small aftershocks, occuring within six minutes of the main San Fernando earthquake, were recorded at Pacoima Dam. In fitting theoretical waveforms to these records, we are able to see some of the limitations of the model due to source-station distance and possible intervening structure. Also, we discuss some of the limitations in our knowledge of the magnitude range of the source parameters.

Finally, Section IV presents a summary of our findings with possible directions of future studies.

SECTION II

A DISCUSSION OF FAULT PARAMETER VARIATION WITHIN HASKELL'S MODEL

A. A ROUGH GUIDE TO THE FAULT PARAMETER VARIATION

In an attempt to better understand the Haskell moving dislocation source, and to increase the efficiency with which the theoretical source is fitted to the empirical data, a study of the effects of the variation of the individual parameters was undertaken. A concise description of the equations derived by Haskell (1969) for computing the theoretical waveforms is given by Tsai and Patton (1973). They also discuss the technique adopted for numerically integrating the Green's function integrals. Briefly, the fault plane area is assumed to be rectangular with length L in the X_1 direction and width W in the X_2 direction as indicated in Figure II-1. Over this surface the shear dislocation is described as:

$$D_i(X_1, X_2, t) = \begin{cases} 0 & t - \frac{X_1}{V} < 0 \\ \frac{D_{io}}{T}(t - X_1/V) & 0 < t - \frac{X_1}{V} < T \\ D_{io} & t - \frac{X_1}{V} > T \end{cases} \quad \text{(II-1)}$$

where i=1 and 2 for longitudinal and transverse shear dislocation respectively. This form of dislocation function implies that at t = 0 a fracture front is established instantaneously over a length W of the X_2 axis. At any fixed point on the fault plane the relative displacement D_i increases at constant velocity from 0 at $t = X_1/V$ to a constant final value, D_{io}, at $t = T + X_1/V$. Here T is referred to as dislocation rise time. The dislocation parameters needed for computation are either derived from existing seismic evidence

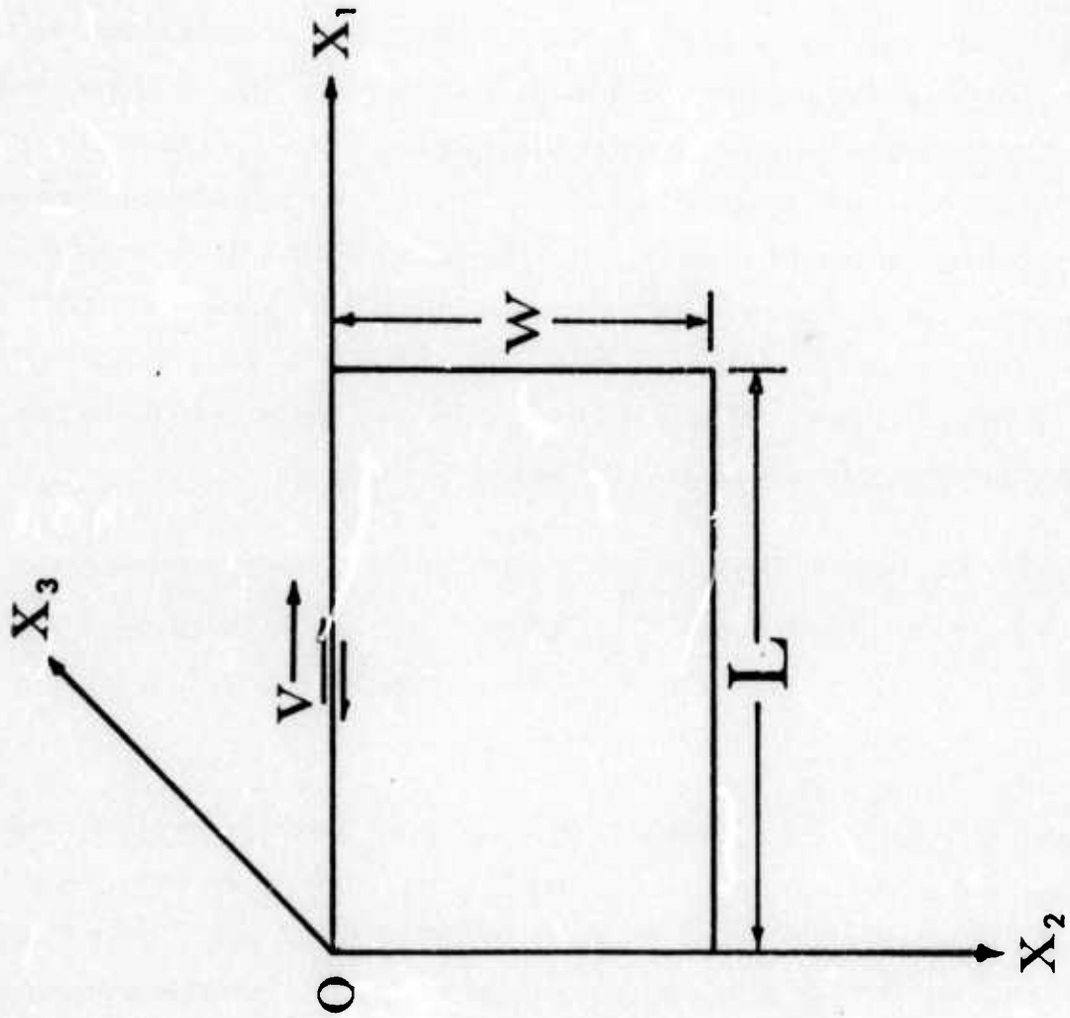

FIGURE II-1

MODEL COORDINATE SYSTEM AND
FAULT PLANE GEOMETRY

such as the fault-plane solution, the aftershock zone, etc., or varied by trial and error until the resultant waveforms are considered to agree substantially with their observed counterparts. In our study, the comparison is accomplished using velocity waveforms. Since this source model is derived for a whole space, the effect of the free surface is approximated by doubling the amplitude of the theoretical waveforms.

The model variables can be divided into two classifications. The first is what may be labeled as non-physical parameters. These are the variables which have no analog in the physical process of fault rupture. They affect the waveform only by determining the convergence of the numerical signal to the analytic solution. The second group, the physical parameters, are those which can actually determine the theoretical waveform. In the following paragraphs, we will present a rough guide of the behavior of the physical parameters.

The physical parameters include the dislocation amplitudes, rise time, rupture velocity, and fault dimensions. In addition, one must include those factors which affect the waveform in a more indirect way, specifically the orientation of the fault surface. This information is contained in the spatial position of the point of evaluation, dip angle, and azimuth. The variation of a physical parameter has extremely subtle effects due to the interrelationships of the parameters. For example, under certain conditions, it is impossible to distinguish between a variation of rise time and rupture velocity. If the position of observation is maintained, a change of the dip angle of the fault plane will rotate the observation point within the displacement field. The same effect could be obtained by holding the dip angle and altering the position of the station.

For some of the parameters, the effects of variation are seen directly from the equations of the model. For either longitudinal or transverse dislocation, the dislocation amplitude can be seen to have only a

scaling effect on the waveform, with no ability to modify the form of either the displacement or velocity signal. In the case of mixed dislocation, the resulting waveform is the superposition of the waves generated by the two modes of dislocation separately. This property gives rise to the use of a least squares technique in amplitude fitting, and this method was used in analyzing the events discussed in this report. This approach yields a measure, through the residuals, of how good our fit of the theoretical to the observed waveform is.

The fault length, the linear dimension in the direction of rupture propagation, and width, the dimension transverse to the rupture, have somewhat similar effects. When one increases the fault area by altering one or both of these dimensions, one increases the source of contributors to the displacement wave. As each elemental area behaves in the same manner, one is merely adding to the amplitude in an almost linear manner. The effect is almost, but not exactly, linear due because the fault plane position is altered with respect to the observation point.

For the fault width, the added width will rupture the same instant as in the original case, but depending on where it is added, it will be either nearer or further away from the observation point. Thus, the displacements caused by this new area will arrive either earlier or later than in the original case. This alters the waveform by changing the interference pattern between contributing sources. This effect is seen mostly by a change in time durations of the waveform segments. However, the geometry of the situation and the amount of area added is exceedingly important in determining the significance of these effects.

The alteration of the fault length has similar effects to those of added fault width, but is both more complex and more significant in determining the signal duration. This results from the addition of area along the direction of rupture propagation. As with the fault width, the new area is contributing

the same signal as a similar area of the original fault and it affects the resulting signal by originating at a different distance from the observation point, but it is also, due to finite rupture velocities, extending the time over which the rupture process occurs.

It should be noticed that an approximation of varying the fault length could be attained by altering rise times, rupture velocity and dislocation amplitudes.

The rise time is that period for which the dislocation at a specific point goes from zero dislocation to the final value. Obviously, this is significant in determining the time characteristics of the waveform. A fast rise time will decrease the time over which the rupture process proceeds. From the equation below,

$$T_{1(Total)} = L_{Fault} * 1/V_{Rupture} + T_{Rise}, \qquad \text{(II-2)}$$

the time duration of the signal is therefore reduced which alters the interference patterns producing the final wave. As the dislocation occurs quicker, the displacement amplitudes are increased.

As was previously mentioned, increasing the rupture velocity, has a similar effect to decreasing fault length. The resulting wave train is condensed in time except for the initial arrival times of the P and S waves. The effect is analogous to alteration of rise time in that the displacement amplitudes are also increased.

A significant effect resulting from the properties of the rise time, rupture velocity, and fault dimensions is the width of the P- and S-wave velocity waveforms. For some given length of the fault, rupture velocity, and rise time, a steady state displacement function will be achieved for some time period (say T_1). From the diagram below,

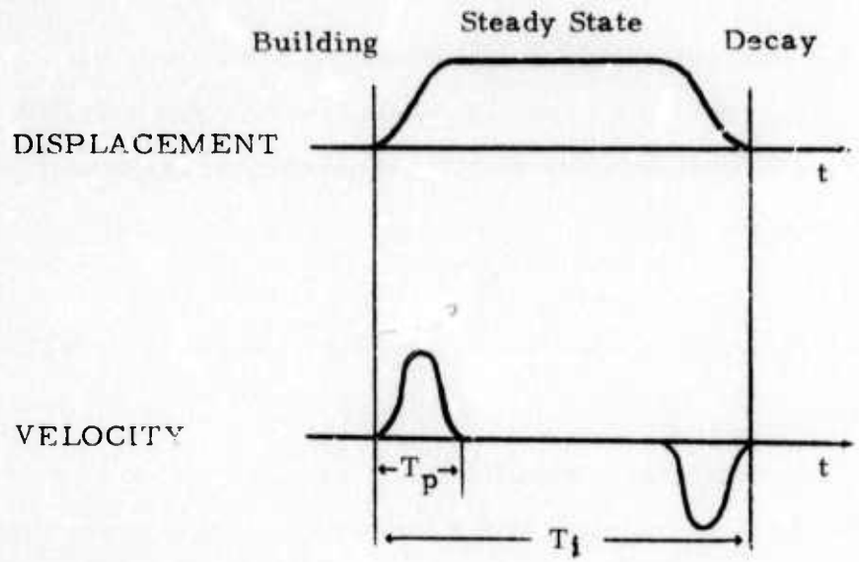

and equation II-1, if we double the fault length, then T_1 becomes significantly longer. We can also reduce V_R to make T_1 grow. The pulse width of the velocity waveform, T_p, is determined by the rise time. Application of these parameters, as well as the affect of the orientation of the fault surface, is discussed in the following paragraphs.

B. A COMPLEX MODEL OF THE SAN FERNANDO EARTHQUAKE

The prime difficulty in any attempt to model a geophysical problem has been in producing a model of sufficient complexity to adequately represent the process while maintaining mathematical tractability. This problem is acute in working with almost any earthquake source description. The incorporation of complexities arising from geologic structure and the use of structural parameters along the rupture surface has been difficult. However, from Tsai and Patton's previous work (1972, 1973) the lack of fit between the observed and theoretical waveforms, in some cases, especially in terms of polarity, indicate that this type of sophistication might be needed.

As originally presented, Haskell's (1969) moving dislocation source mechanism does not include the previously mentioned refinements.

The rupture surface is assumed to be of rectangular geometry, with constant structural parameters, located within a homogeneous whole space. The success with which Tsai and Patton were able to obtain solutions in several cases, with the source parameters comparable with those obtained using independent techniques, indicates that the model does behave well, at least on a first order level.

While the inclusion of any geologic structure into this model would be a formidable task, the model is readily adapted to increased complications in the source mechanism itself, such as stick-slip. Complex source mechanisms may be developed from the simple model by considering a fault configuration to be divided into a series of smaller contiguious fault segments, each having its own set of parameters, such as rupture velocity, dislocation amplitude, dip angle, or width. By summing the displacement or velocity waveforms calculated for each segment with appropriate time delays, which are determined by the arrival of the rupture front at the fault segments, the displacement and velocity waveform of a more complex source mechanism is obtained. By increasing the number of segments, one can derive an earthquake source mechanism of almost any desired complexity. With this in mind, we shall attempt to re-evaluate the San Fernando earthquake source mechanism as determined from the Pacoima Dam record.

Tsai and Patton (1973) reported a solution for this event based on a rectangular fault with a dip of 52^{o}, a fault length of 16.5 km, and fault width of 14.0 km, all of which were based on evidence from other sources. To fit the theoretical waveform, a rupture velocity of 3.0 km/sec, longitudinal and transverse dislocation amplitudes of 200.0 and 10 cm respectively, and a rise time of 0.6 seconds were required. The fit obtained for the records at Pacoima Dam are shown in Figure II-2.

There are two significant variations between the empirical and theoretical waveforms which might be thought to be correctable using a

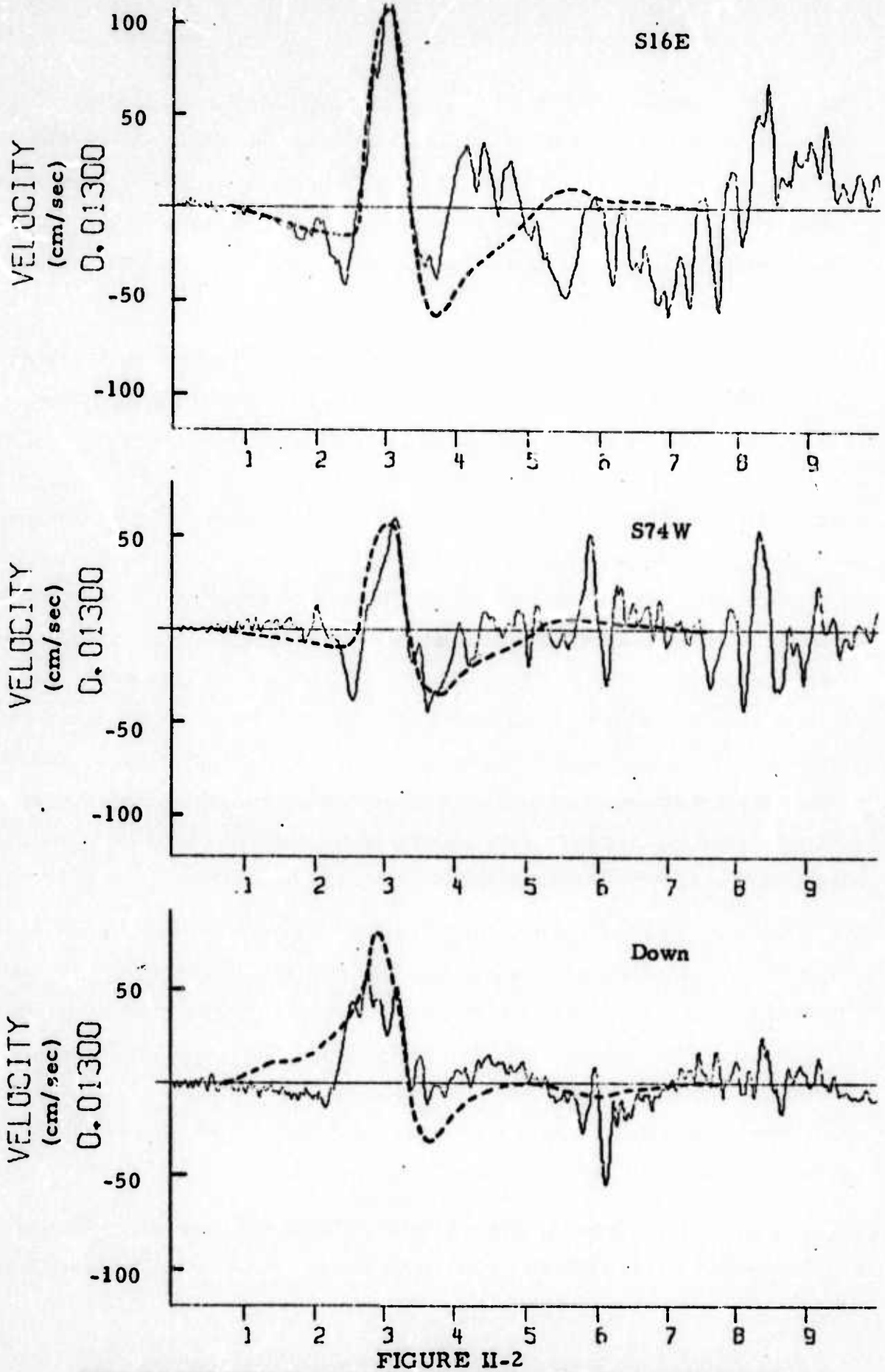

FIGURE II-2
THE OBSERVED (IN SOLID CURVES) AND THE THEORETICAL (IN DASHED CURVES) VELOCITY WAVEFORMS OF THE SAN FERNANDO EARTHQUAKE AS SEEN AT THE PACOIMA DAM

more complex mechanism than originally applied. The first of these features is the initial trend of the vertical waveform. On the observed waveform of the S-wave, the trend is negative prior to the arrival of the main pulse. However, the theoretical fit demonstrates a positive initial trend. Secondly, while the main horizontal pulse amplitudes are fitted reasonably well, the amplitudes and duration of the theoretical wave, exclusive of the main pulse, show significant deviations from the empirical waveform.

Initial work was carried out to determine the effects of a stick-slip mechanism as compared to the constant rupture velocity model as utilized by Tsai and Patton (1973). As was indicated in the review of parameter variations, the variation of the rupture velocity has a uniform effect on the time durations of the waveforms, compressing or lengthening the waveform without effecting the basic shape or polarities, and a uniform effect on all the component amplitudes. If one were to run the stick-slip model with the same rupture velocity in each segment of the fault, the resulting waveform would be virtually identical to the model used by Tsai and Patton (1973). However, by altering the rupture velocity, one can control the time durations of individual segments contributing to the final waveform. In turn, by controlling the time duration of the waveform of the fault segment which dominates a particular section of the final signal, one can control the duration of a single portion of the final waveform.

In addition, the variation of rupture velocity alters the time relationships between contributions of certain points on the fault plane to the waveform. For example, by decreasing the rupture velocity of a central segment, the last segment will not even start to rupture until some time later than in the constant velocity case. Thus, the patterns of destructive and constructive interference within the waveform are altered, affecting the final signal form. It was evident, though, after conducting several cases, that the effect of a stick-slip model, when constrained to physically reasonable

rupture velocities (Johnson, et al 1973), was not enough to radically alter the resulting waveform. In order to significantly alter the solution, it was concluded that a more complex source mechanism, in terms of geometry and the other fault parameters, would be needed.

Other investigators have demonstrated that the fault surface that ruptured during the San Fernando earthquake was non-planar. Both Jungles and Frazier (1973), using static dislocations, and Whitcomb, et al (1973), using aftershock fault plane solutions, indicate that the rupture surface is hinged, having one dip angle above a point 6 km over the hypocenter, and another dip angle below that point. In addition, there is no reason to assume a constant fault width, dislocation amplitude, or rise time. Thus, by allowing these parameters to vary, a new solution to the main event of the San Fernando earthquake can be generated.

In the beginning of our analysis, it was intended that the Jungles and Frazier would be used as the basis for a re-evaluation of the Pacoima Dam accelerograms using complex source configurations of the Haskell moving dislocation source. It soon became evident, though, that the number of fault segments needed to adequately describe this model, eleven, with the associated 66 parameters, was unmanagable considering the degree of refinement expected for the solution. However, the initial work done with this model established certain properties which are worthy of note.

The dislocation amplitudes and the fault structure of this model do produce a waveform reasonably close to the velocity wave calculated from the Pacoima Dam accelerograms. But, even without taking into account a free surface effect, the waveform amplitudes are approximately three times too great. For example, in the upper fault segment, where Jungles and Frazier estimate an 8.3 meter dislocation, we find a 2.7 meter dislocation. Similar reductions are necessary along the entire fault surface to produce waveform amplitudes approximating those of the empirical data. These

waveforms are shown in Figure II-3, with a cross-section of the structure given in Figure II-4 and a tabulation of the parameters for each segment given in Table II-1.

Our solution should be compared to Jungles' and Frazier's considering the following assumptions. First, the analytical descriptions of the source are quite different. They use a finite element variational method to our Haskell dynamic dislocation. Secondly, they use a heterogeneous half-space accounting for local geology, while we use a homogeneous whole space with an approximation used to account for the free surface. The primary objectives of this comparison was to get some feeling for the idealizations inherent in the Haskell model, and the analysis of a segmented fault structure. Also, in judging the comparison, we should keep in mind the possible non-uniqueness of Jungles' and Frazier's local geology and our description of the source-time function (choice of rise time, rupture velocity, etc.).

Keeping these assumptions in mind, and still desiring to determine the effects of a segmented fault plane, a simplified model of only five segments was chosen. The fitted waveform for this model is shown in Figure II-5, with a cross-section of the structure given in Figure II-6 and a tabulation of the parameters for each segment given in Table II-2. One of the most significant variations of the waveform results from the hinged fault structure. In the Tsai and Patton's (1973) uniform model, the vertical S-wave trace of the velocity signal has an initial positive trend. The hinged fault surface, though, produces an initial negative trend similar to that of the observed vertical trace.

The improved fit resulting from the hinged fault surface encouraged us to make further adjustments to the model. After varying the width, rupture velocity, length, and longitudinal dislocation of each segment, a better fit was obtained in terms of pulse width and amplitude (compare

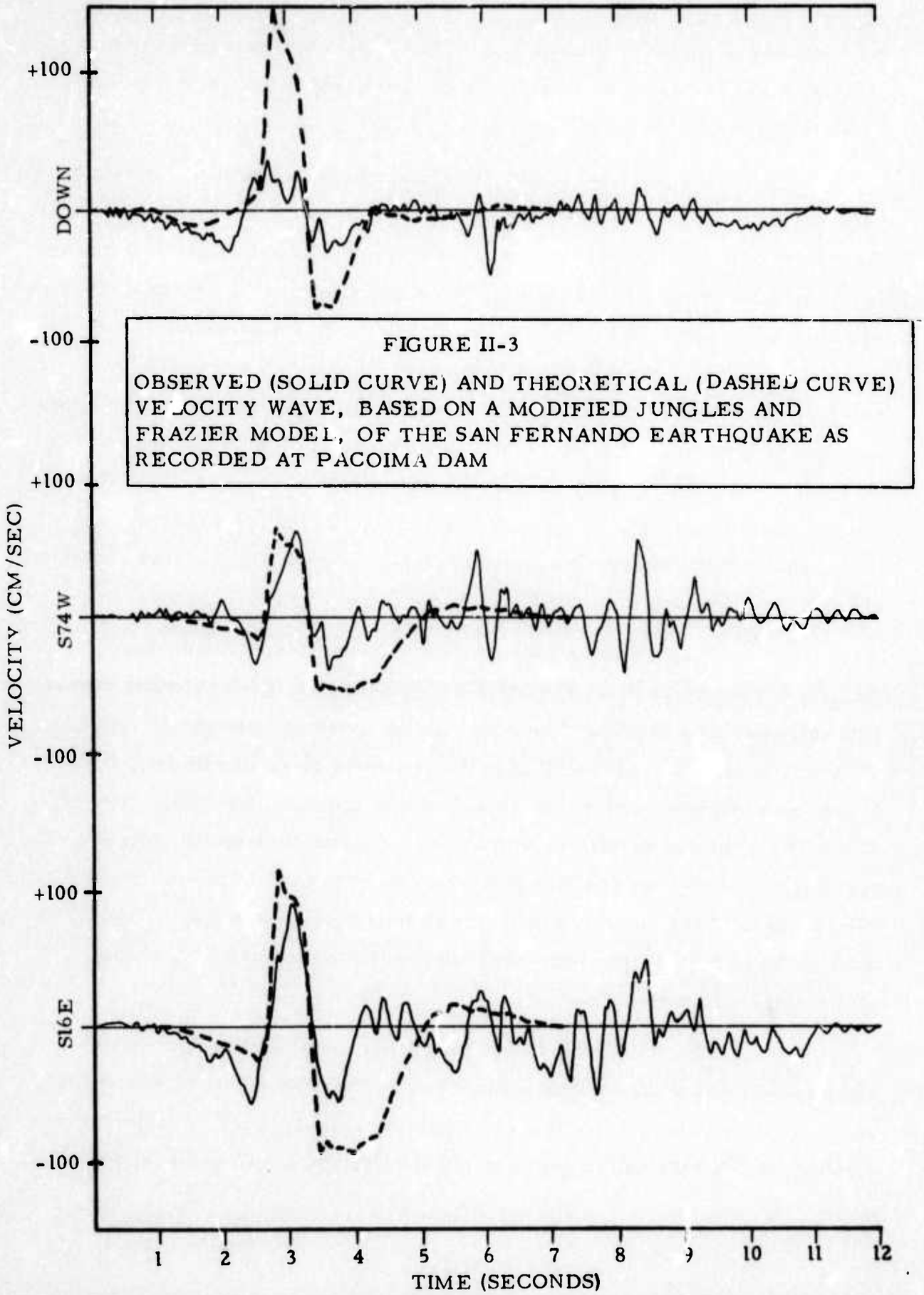

FIGURE II-3

OBSERVED (SOLID CURVE) AND THEORETICAL (DASHED CURVE) VELOCITY WAVE, BASED ON A MODIFIED JUNGLES AND FRAZIER MODEL, OF THE SAN FERNANDO EARTHQUAKE AS RECORDED AT PACOIMA DAM

SAN FERNANDO EARTHQUAKE MODIFIED JUNGLES AND FRAZIER MODEL

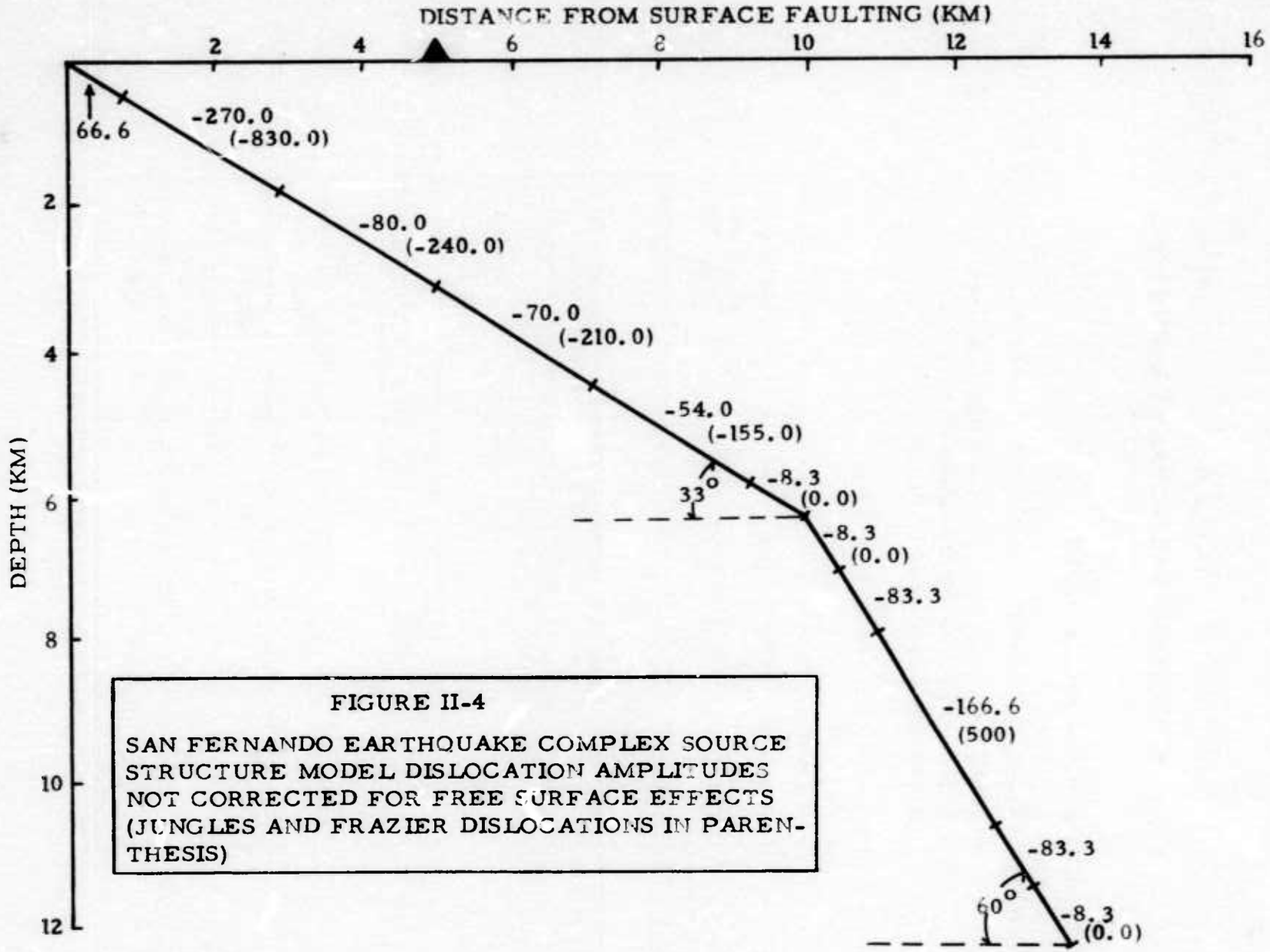

FIGURE II-4

SAN FERNANDO EARTHQUAKE COMPLEX SOURCE STRUCTURE MODEL DISLOCATION AMPLITUDES NOT CORRECTED FOR FREE SURFACE EFFECTS (JUNGLES AND FRAZIER DISLOCATIONS IN PARENTHESIS)

TABLE II-1

SAN FERNANDO EARTHQUAKE - MAIN EVENT

Modified Jungles and Frazier Model

Constants: V_P = 5.5 km/sec V_S = 3.2 km/sec
Width = 14.0 km Rise Time = 0.6 sec
Rupture Velocity = 3.0 km/sec
Transverse Dislocation = 0.0 cm

Starting with segment nearest hypocenter.

Segment	Dip	Length (km)	Longitudinal Dislocation (cm)*
1	60°	1.0	-8.33
2	60°	1.0	-83.3
3	60°	3.044	-166.7
4	60°	1.0	-83.3
5	60°	1.0	-8.33
6	33°	0.8	-8.33
7	33°	2.5	-54.52
8	33°	2.5	-70.0
9	33°	2.5	-80.0
10	33°	2.5	-270.0
11	33°	1.0	-66.6

*Not corrected for free surface effect.

Figures II-2 and II-5). As implied in our previous discussion, these choices are not unique, but give an indication of the adaptability of the model under different fault configurations.

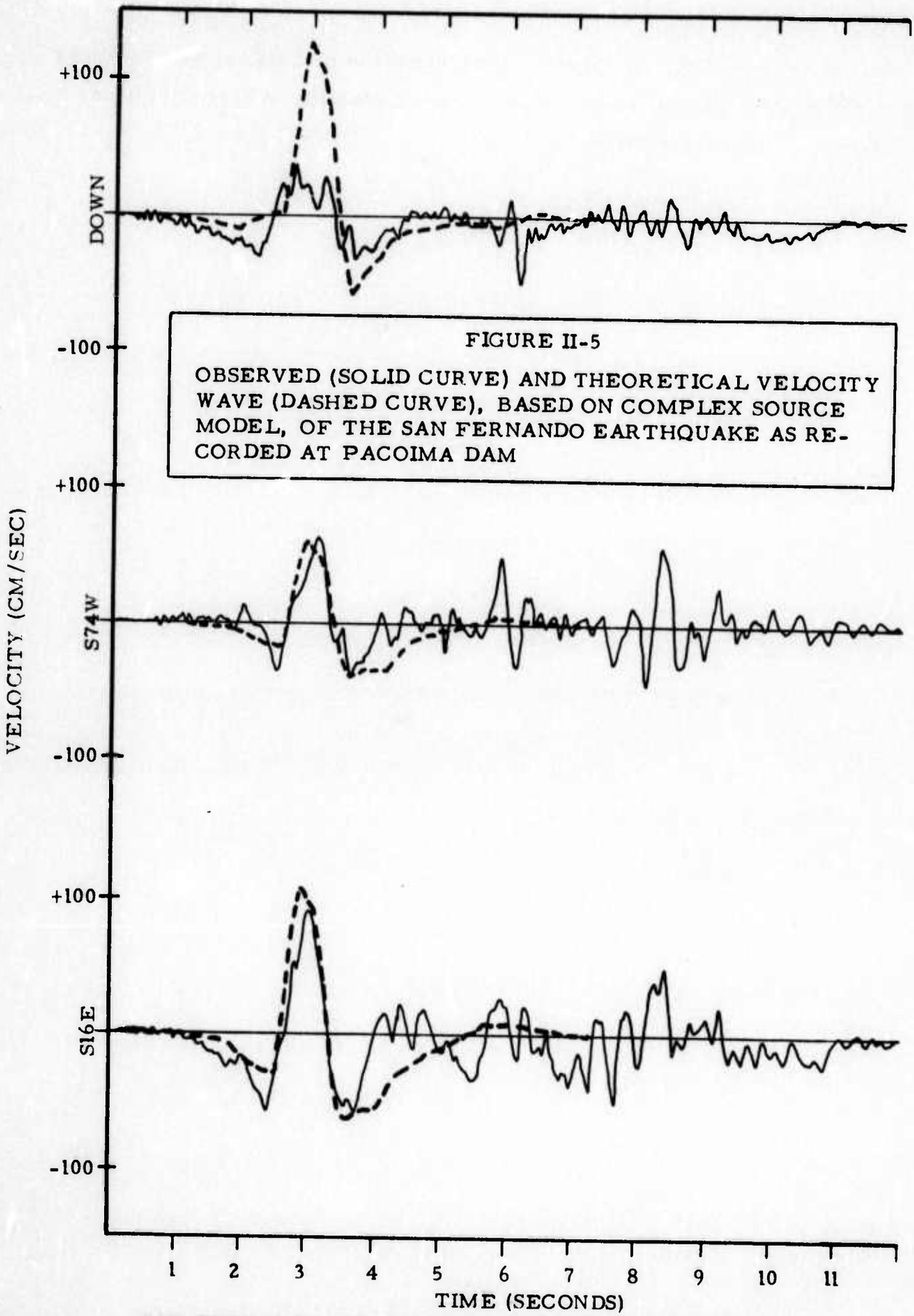

FIGURE II-5

OBSERVED (SOLID CURVE) AND THEORETICAL VELOCITY WAVE (DASHED CURVE), BASED ON COMPLEX SOURCE MODEL, OF THE SAN FERNANDO EARTHQUAKE AS RECORDED AT PACOIMA DAM

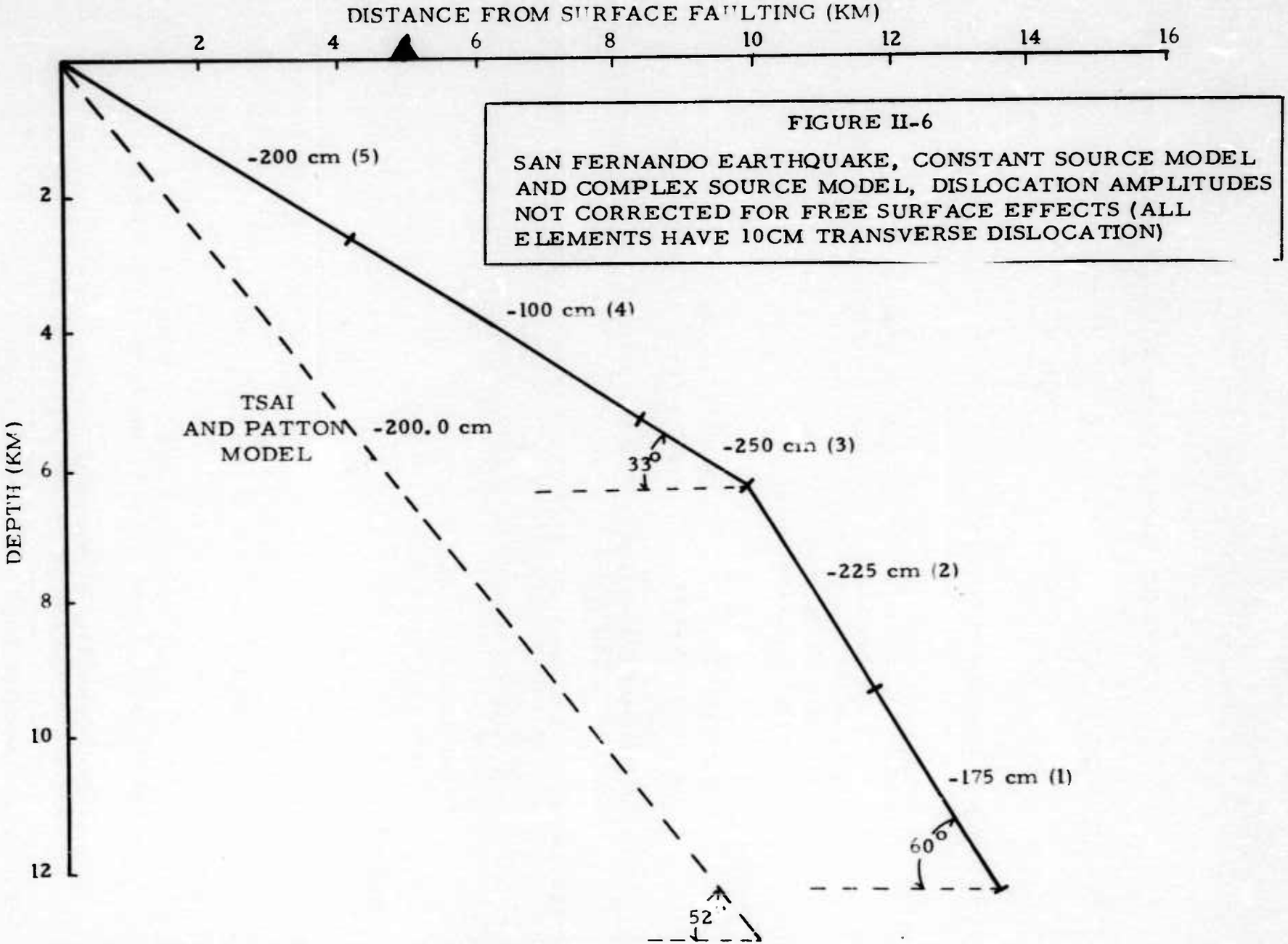

FIGURE II-6

SAN FERNANDO EARTHQUAKE, CONSTANT SOURCE MODEL AND COMPLEX SOURCE MODEL, DISLOCATION AMPLITUDES NOT CORRECTED FOR FREE SURFACE EFFECTS (ALL ELEMENTS HAVE 10CM TRANSVERSE DISLOCATION)

TABLE II-2

SAN FERNANDO EARTHQUAKE - MAIN EVENT

Complex Source Model*

Constants: V_P = 5.5 km/sec V_S = 3.2 km/sec

Starting with Segments at Hypocenter

Segment 1

Width = 12.0 km Length = 3.5 km
Rise Time = 0.6 sec Rupture Velocity = 3.0 km/sec
Dip = 60°
Longitudinal Dislocation = -175 cm
Transverse Dislocation = -10 cm

Segment 2

Width = 14.0 km Length = 3.5 km
Rise Time = 0.60 sec Rupture Velocity = 2.88 km/sec
Dip = 60°
Longitudinal Dislocation = -225 cm
Transverse Dislocation = -10 cm

Segment 3

Width = 16.0 km Length = 1.8 km
Rise Time = 0.6 sec Rupture Velocity = 2.85 km/sec
Dip = 33°
Longitudinal Dislocation = -250 cm
Transverse Dislocation = -10 cm

Segment 4

Width = 14.0 km Length - 5.0 km
Rise Time = 0.6 sec Rupture Velocity = 3.00
Dip = 33°
Longitudinal Dislocation = -100 cm
Transverse Dislocation = -10 cm

Segment 5

Width = 12.0 km Length = 5.0 km
Rise Time = 0.6 sec Rupture Velocity =3.20 km/sec
Dip = 33°
Longitudinal Dislocation = -200 cm
Transverse Dislocation = -10 cm

*Dislocations not corrected for free surface effect.

SECTION III

ANALYSIS OF THREE AFTERSHOCKS IN THE SAN FERNANDO EVENT SEQUENCE

Triggered by the initial shock of the San Fernando earthquake, the strong-motion accelerograph at Pacoima Dam continued to operate for a period of approximately 320 seconds after the main event. During this time, over 30 aftershocks occurring in the near-field were recorded by these instruments. Using Haskell's moving dislocation, Tsai and Patton (1973) have analyzed the first aftershock of this sequence. Since their work, three more events from this series have been interpreted. These events are identified by numbers 4, 11, and 30, using the notation of Trifunac (1972). The first motions of these aftershocks were recorded at approximately 70, 124, and 310 seconds after recording began (Figures III-1).

The initial step in fitting these aftershocks was to determine approximate positions of their hypocenters. In the analysis of the first aftershock, Tsai and Patton (1973) restricted the location of the event to a volume directly on or above the fault plane of the main shock (Figure III-2). However, for subsequent aftershocks, this was determined to be too limited a range of positions to fit these events. Instead, our location estimates were based on the S- minus P-wave arrival time difference determined from the velocity wave, and the relative polarities of the three components. Assuming a simple double couple source with the same mechanism as the main event, the aftershock was limited to one quadrant with respect to the recording station. The position of the event within this quadrant was varied until a satisfactory waveform fit was obtained. The locations obtained by Trifunac (1972) using S- minus P-wave times, were used for initial epicentral positions. The depth for each aftershock was then determined by the S- minus P-wave

FIGURE III-1A

PACOIMA DAM STRONG MOTION ACCELEROGRAM, SHEET 1
SAN FERNANDO, CALIFORNIA, EARTHQUAKE OF FEBRUARY 9, 1971
SHOWING MAIN SHOCK AND EVENT 4

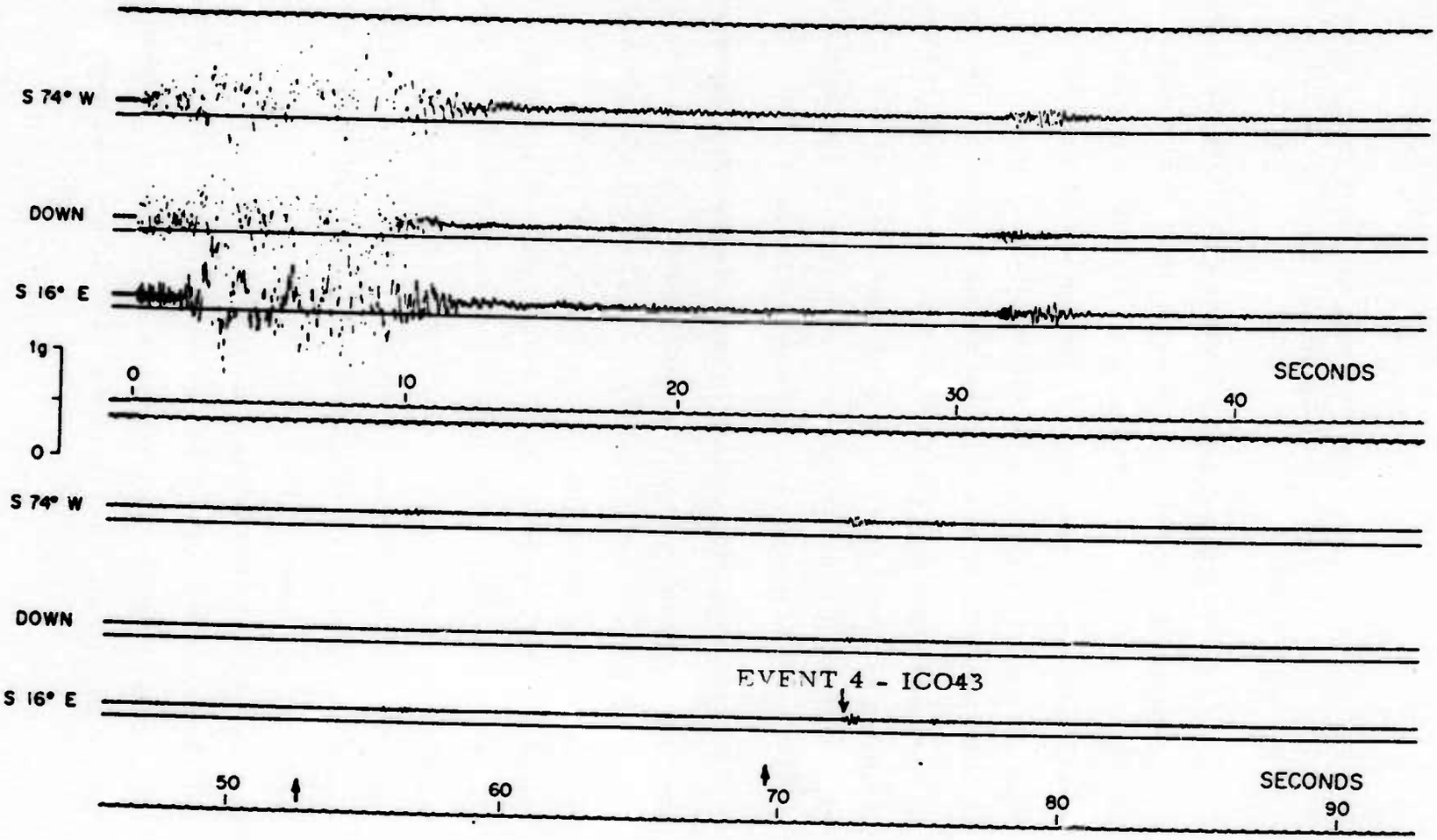

FIGURE III-1B

PACOIMA DAM STRONG MOTION ACCELEROGRAM, SHEET 2
SAN FERNANDO, CALIFORNIA, EARTHQUAKE OF FEBRUARY 9, 1971
SHOWING EVENT 11

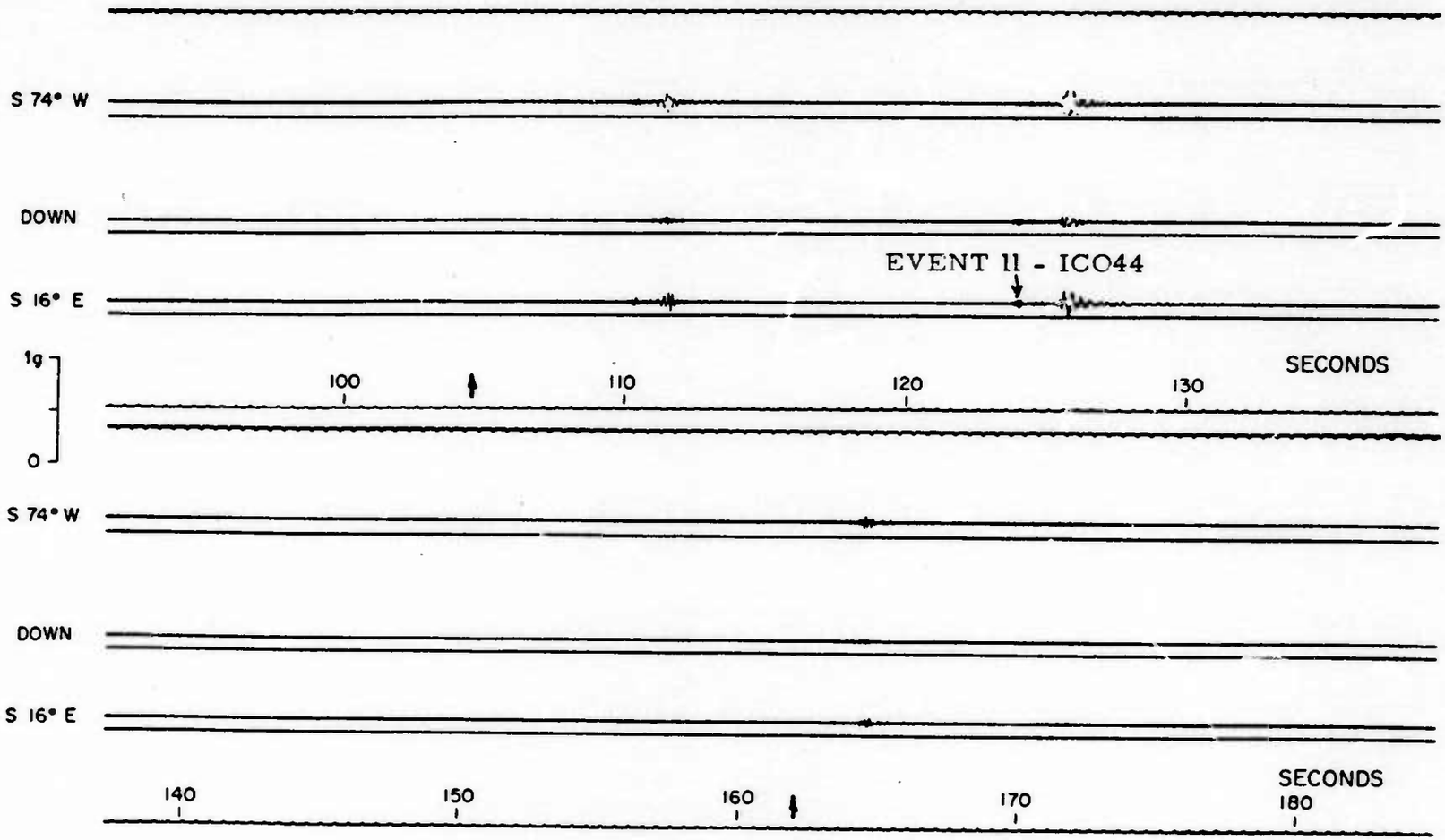

FIGURE III-1C

PACOIMA DAM STRONG MOTION ACCELEROGRAM, SHEET 4
SAN FERNANDO, CALIFORNIA, EARTHQUAKE OF FEBRUARY 9, 1971
SHOWING EVENT 30

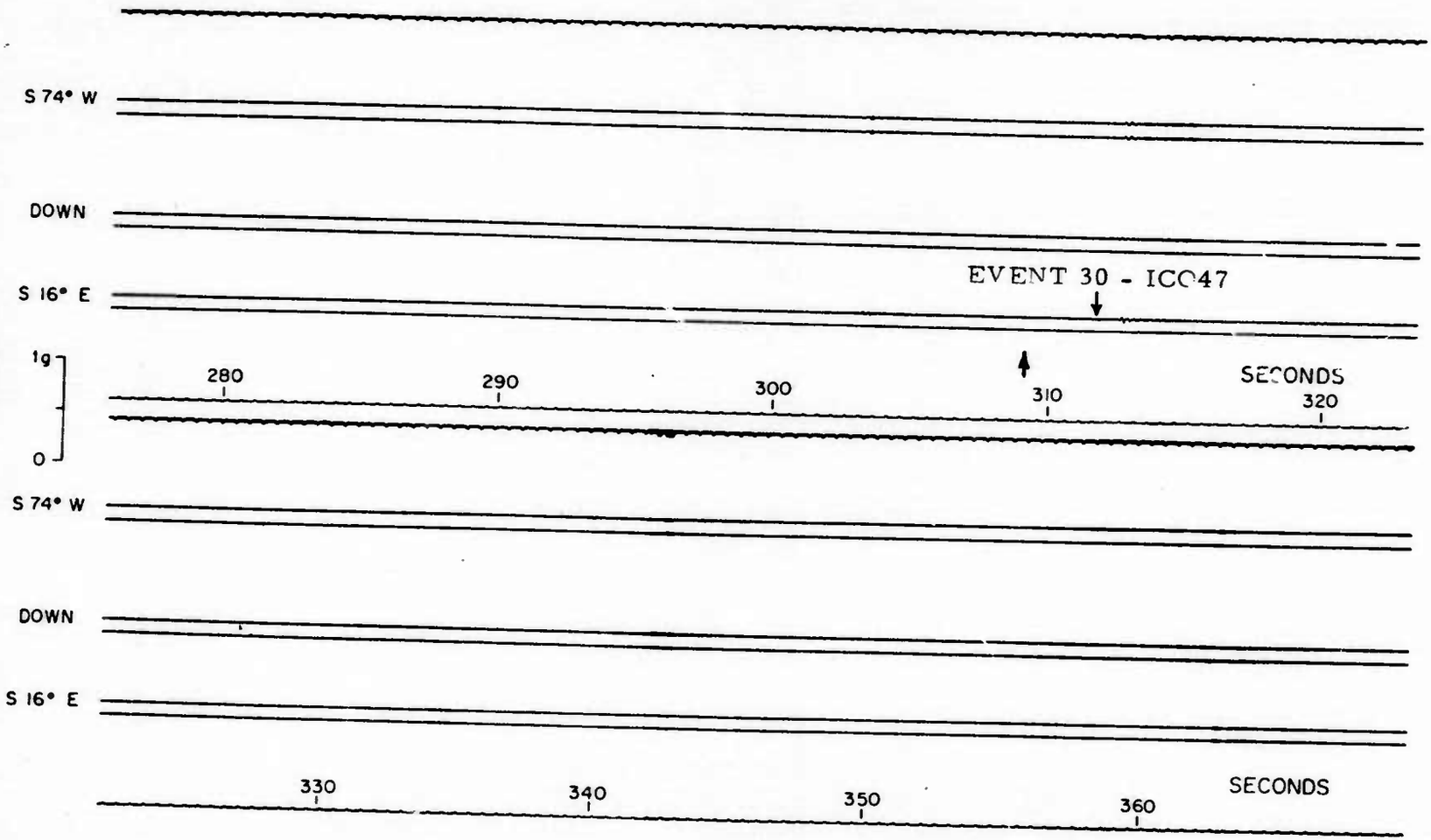

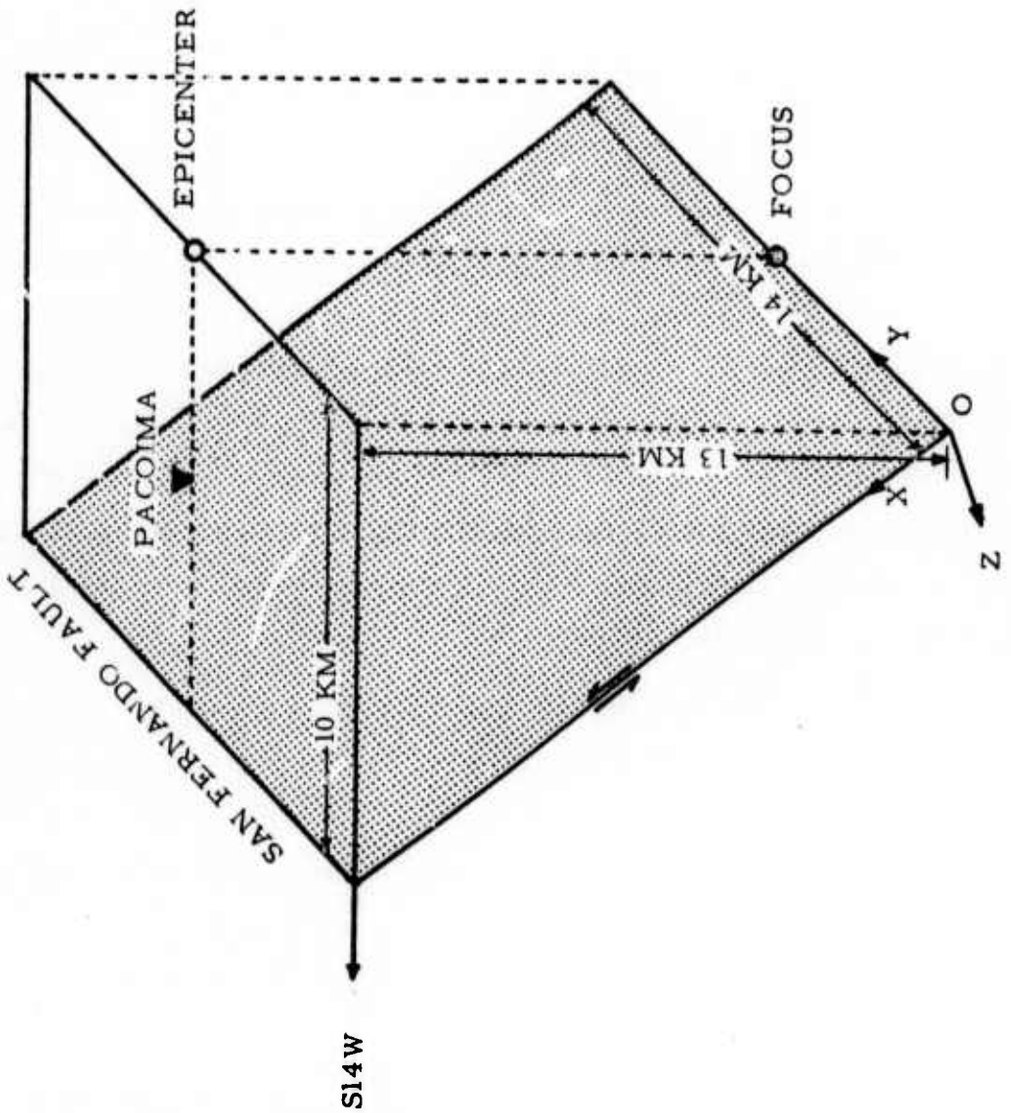

FIGURE III-2

GEOMETRY OF FAULT PLANE BY WHICH TSAI AND PATTON RESTRICTED LOCATIONS OF AFTERSHOCKS OF THE SAN FERNANDO EARTHQUAKE

time recorded at Pacoima Dam. Comparison of our locations with those of Trifunac's (1972) is shown in Figure III-3, and their location on the fault model surface determined by Whitcomb (1973) is given by Figure III-4.

At this point, a decision was necessary to determine what segment of the velocity waveform was to be fitted. Obviously, it is required that the S- minus P-wave time and the P-wave polarities be matched. However, the theoretical waveform does not display any affects of either geologic structure or the free surface. Thus, it is considerably less complex than the empirical wave.

Since the major part of the fitting process involves matching the S-wave, the empirical data must be simplified to allow comparison with the theoretical wave. We assumed that the information describing the dominent rupture phenomenon of a particular aftershock was contained in the wavelet with the greatest peak-to-peak amplitude on the horizontal components. Thus, it was felt that it would be most appropriate to fit this wavelet for all the components. In some cases, the second pulse of the wavelet had been affected by interference. In these cases, it was attempted to reconstruct by eye the original waveform (Figure III-6b).

Once the decision had been made to fit a particular part of the S-wave, theoretical waveforms were generated for various source parameters until the desired relative amplitudes, polarities, and pulse widths could be produced. These initial runs were evaluated with unity dislocation amplitudes for both the longitudinal and transverse dislocations. The least squares fitting routine, mentioned earlier, provided the 'best-fit' dislocation amplitudes.

Using these techniques, solutions for the three aftershocks were determined. The accelerograms and fitted velocity waveforms of events 4, 11, and 30 are shown in Figures III-5, III-6, and III-7 respectively. A summary of these solutions is given in Table III-1, with the parameter values

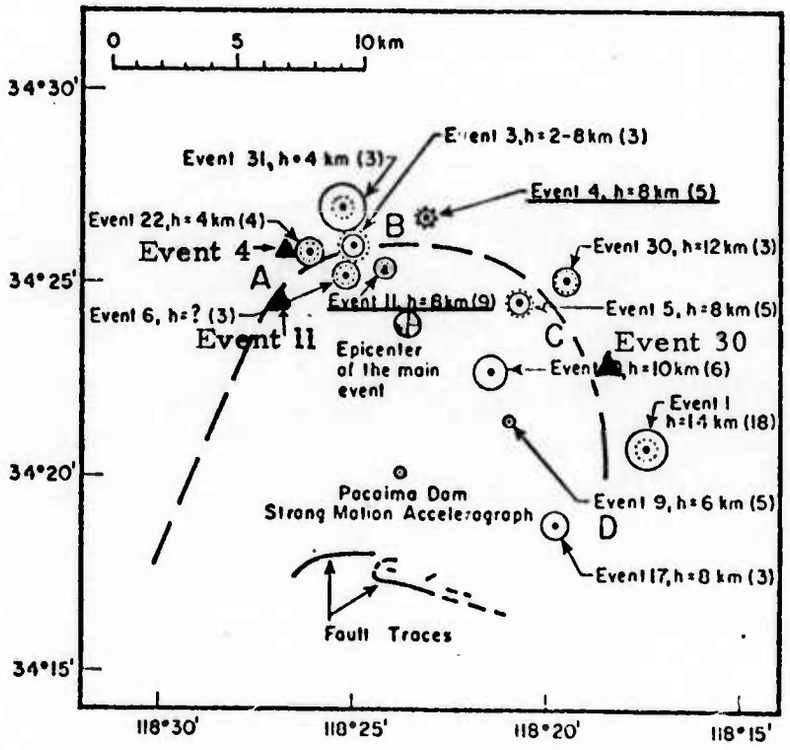

FIGURE III-3

AFTERSHOCKS OF THE SAN FERNANDO EARTHQUAKE, LOCATIONS BY TRIFUNAC (OPEN CIRCLES) AND LOCATIONS BY DISLOCATION MODEL (TRIANGLES). MAIN EVENT FAULT SURFACE INDICATED BY DASHED LINE

FIGURE III-4

LOCATIONS OF AFTERSHOCKS OF SAN FERNANDO EARTHQUAKE (TRIFUNAC - HEXAGONS, HASKELL MODEL SOLUTIONS - CIRCLES) SUPERIMPOSED ON WHITCOMB FAULT SURFACE MODEL

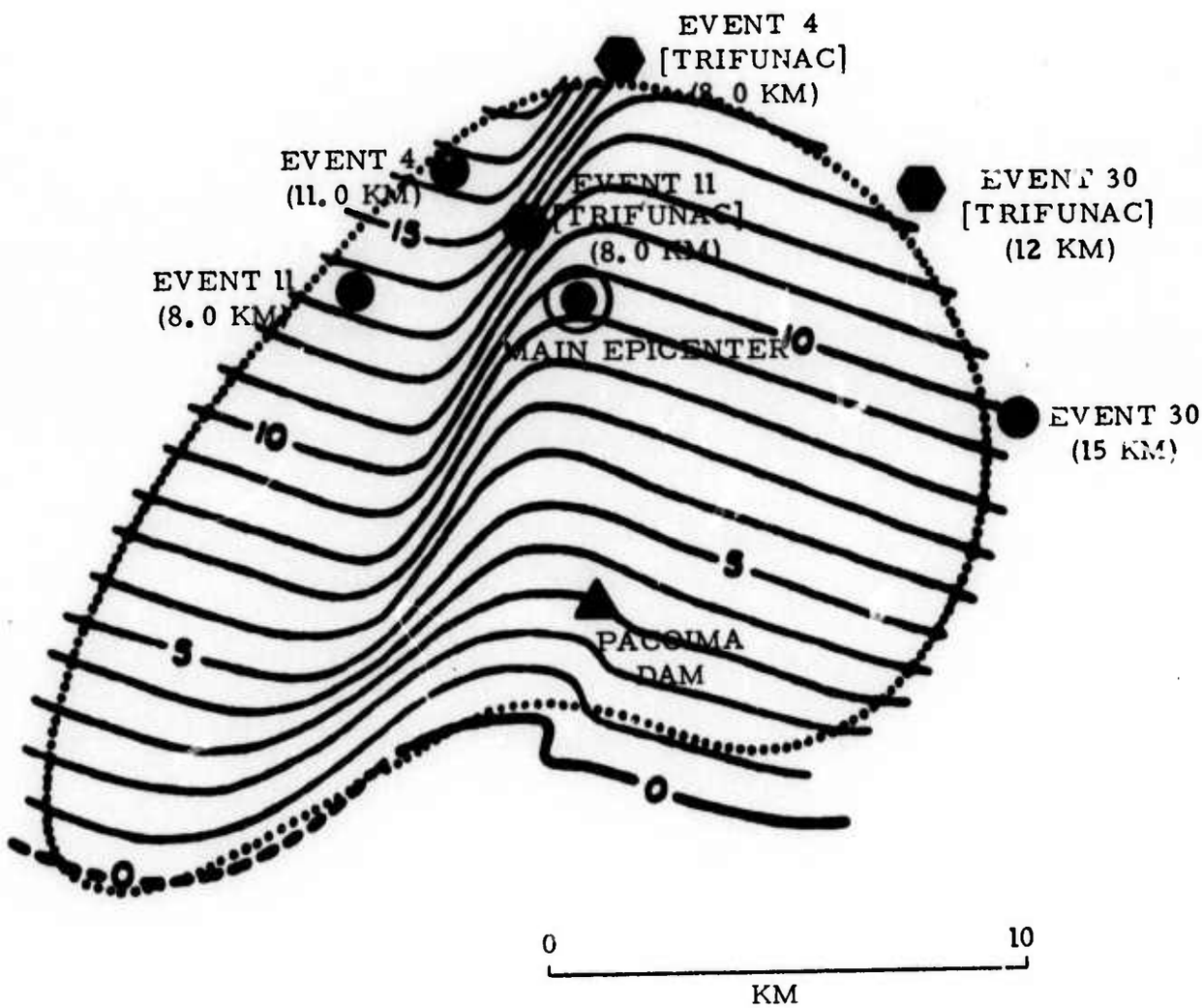

AFTERSHOCK LOCATIONS
WHITCOMB FAULT SURFACE MODEL

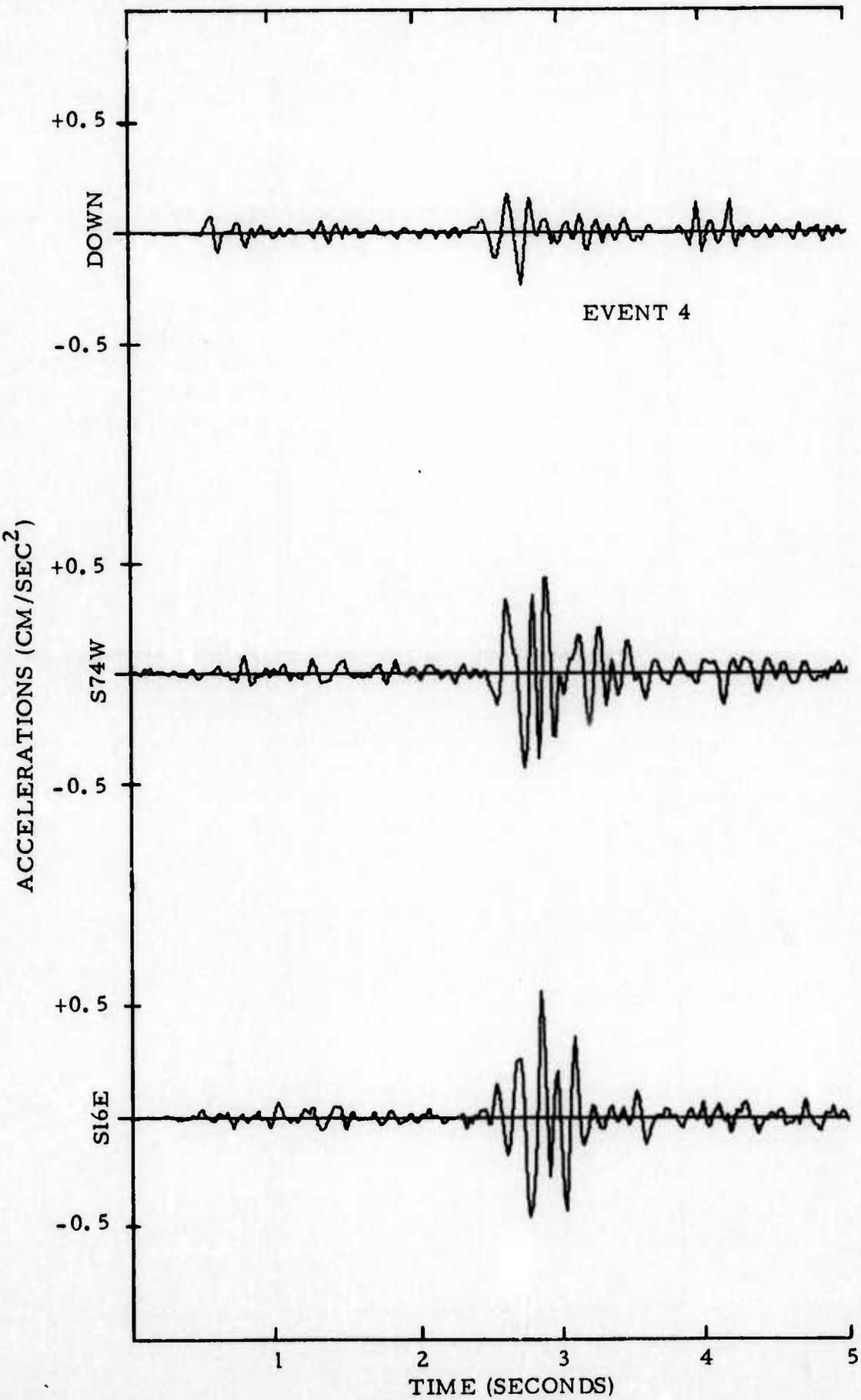

FIGURE III-5A

ACCELERATION TRACES OF EVENT 4, AN AFTERSHOCK OF THE SAN FERNANDO EARTHQUAKE, AS RECORDED AT PACOIMA DAM

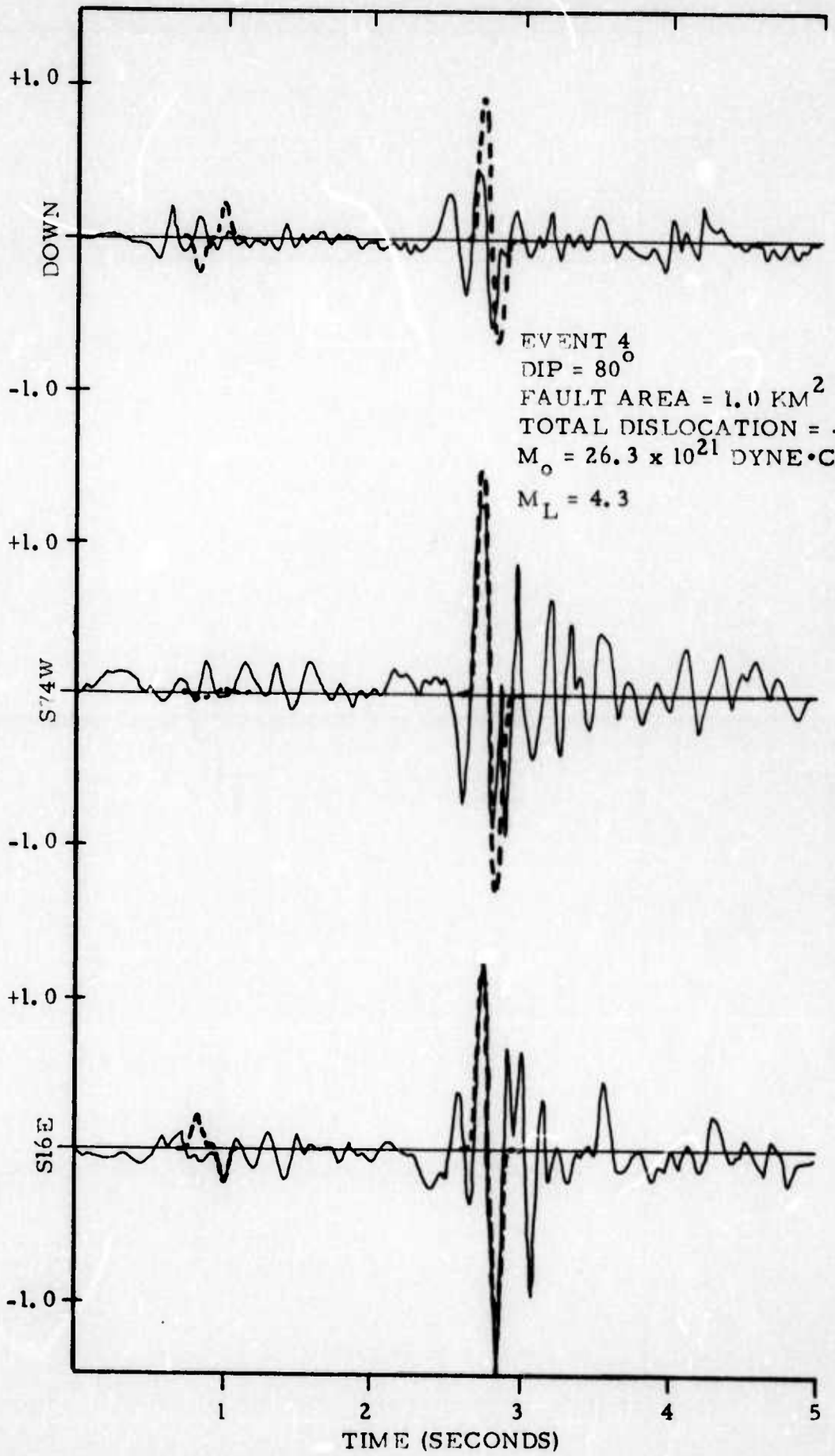

FIGURE III-5B

OBSERVED (SOLID CURVE) AND THEORETICAL (DASHED CURVE) VELOCITY WAVE OF EVENT 4 AS RECORDED AT PACOIMA DAM

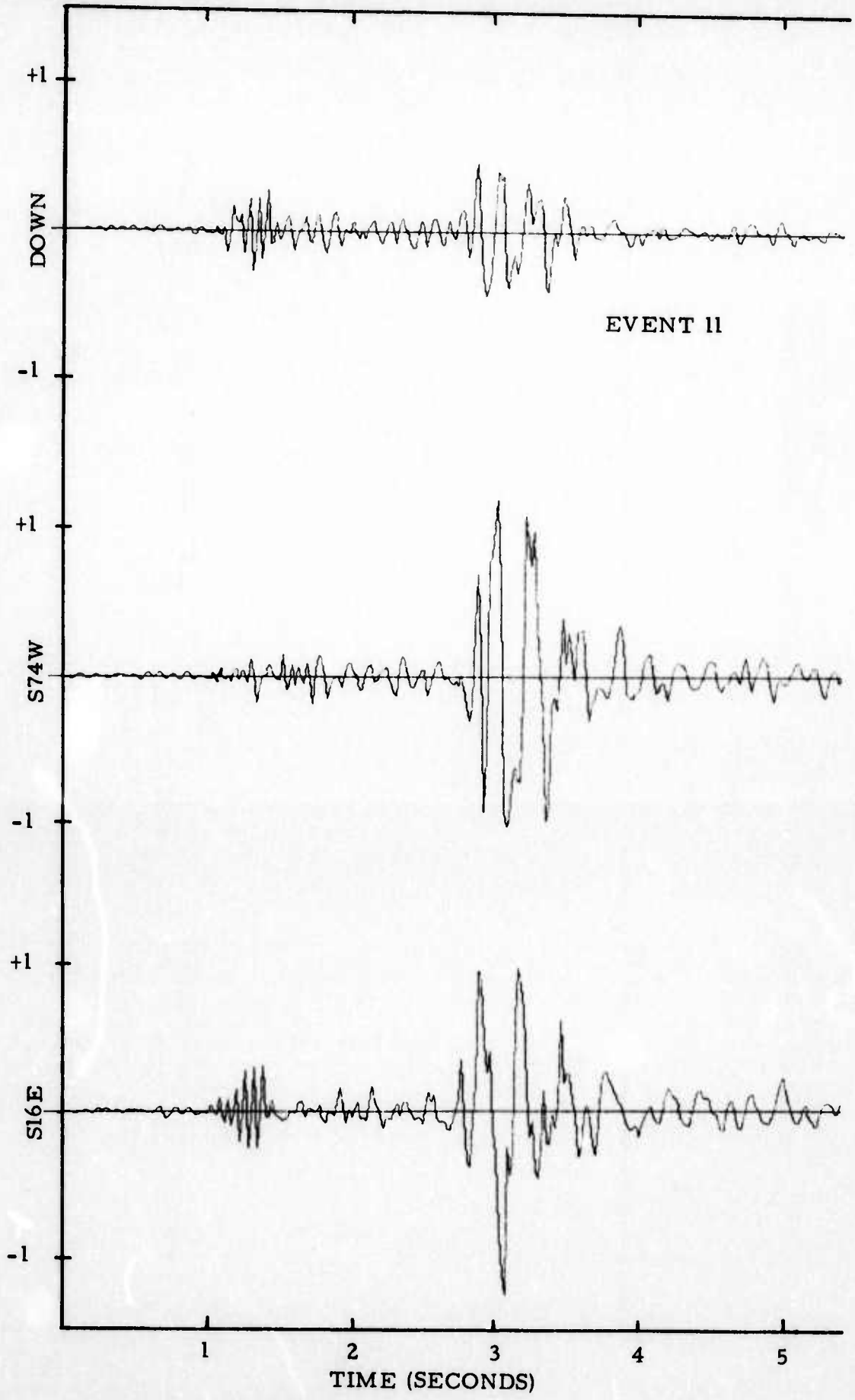

FIGURE III-6A

ACCELERATION TRACES OF EVENT 11, AN AFTERSHOCK OF THE SAN FERNANDO EARTHQUAKE, AS RECORDED AT PACOIMA DAM

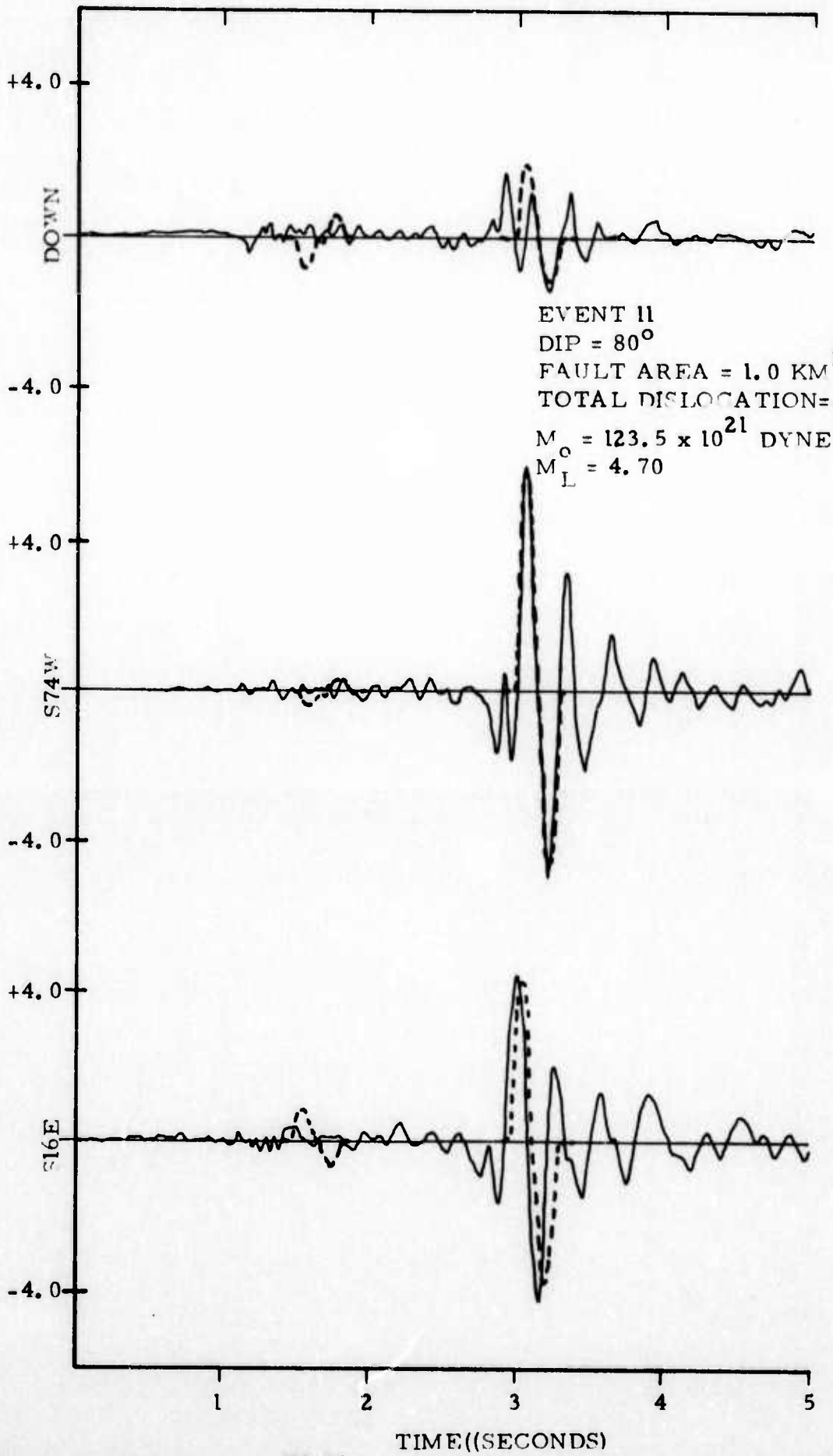

FIGURE III-6B

OBSERVED (SOLID CURVE) AND THEORETICAL (DASHED CURVE) VELOCITY WAVE OF EVENT 11 AS RECORDED AT PACOIMA DAM

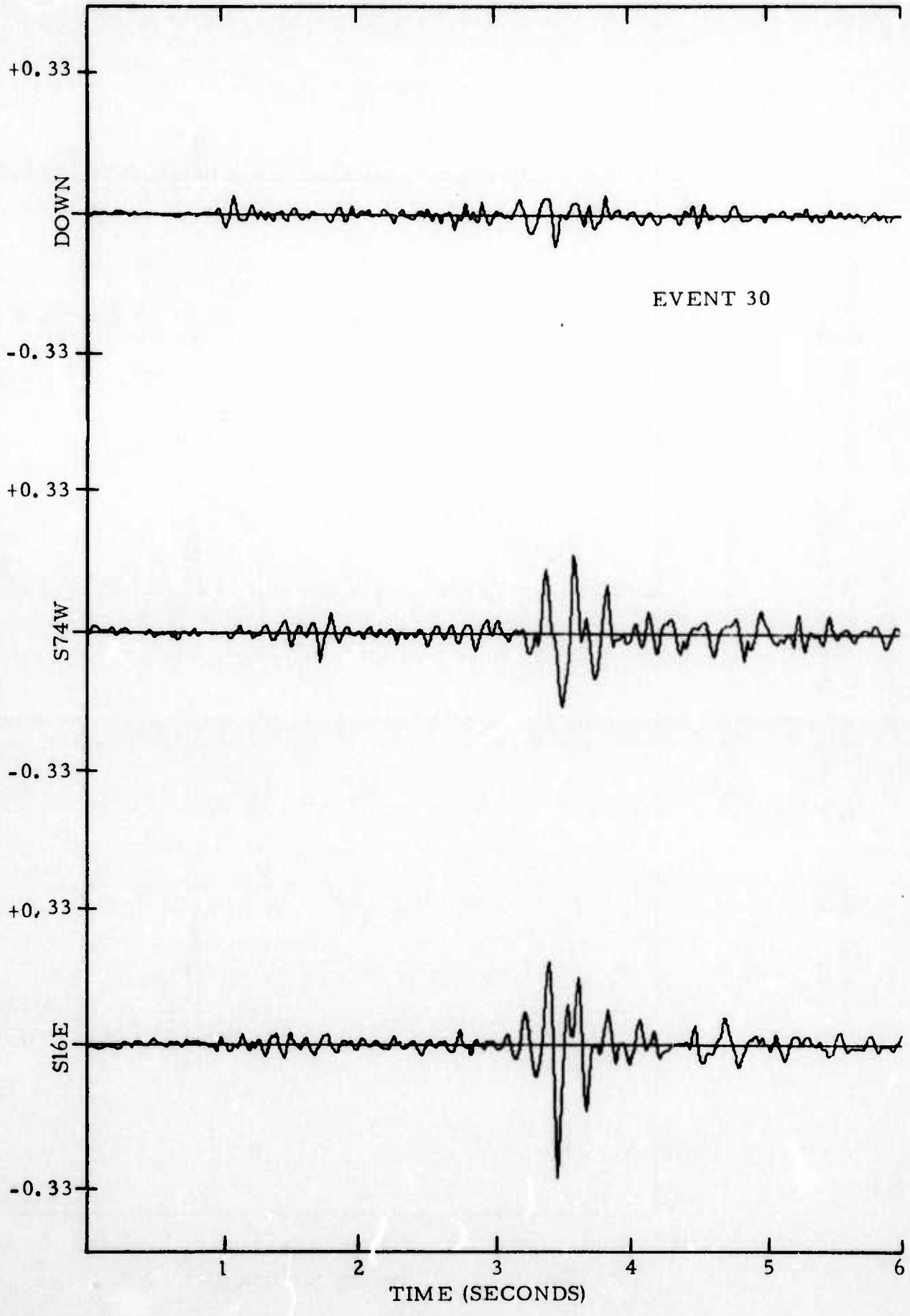

FIGURE III-7A

ACCELERATION TRACES OF EVENT 30, AN AFTERSHOCK OF THE SAN FERNANDO EARTHQUAKE, AS RECORDED AT PACOIMA DAM

ACCELERATIONS (CM/SEC^2)

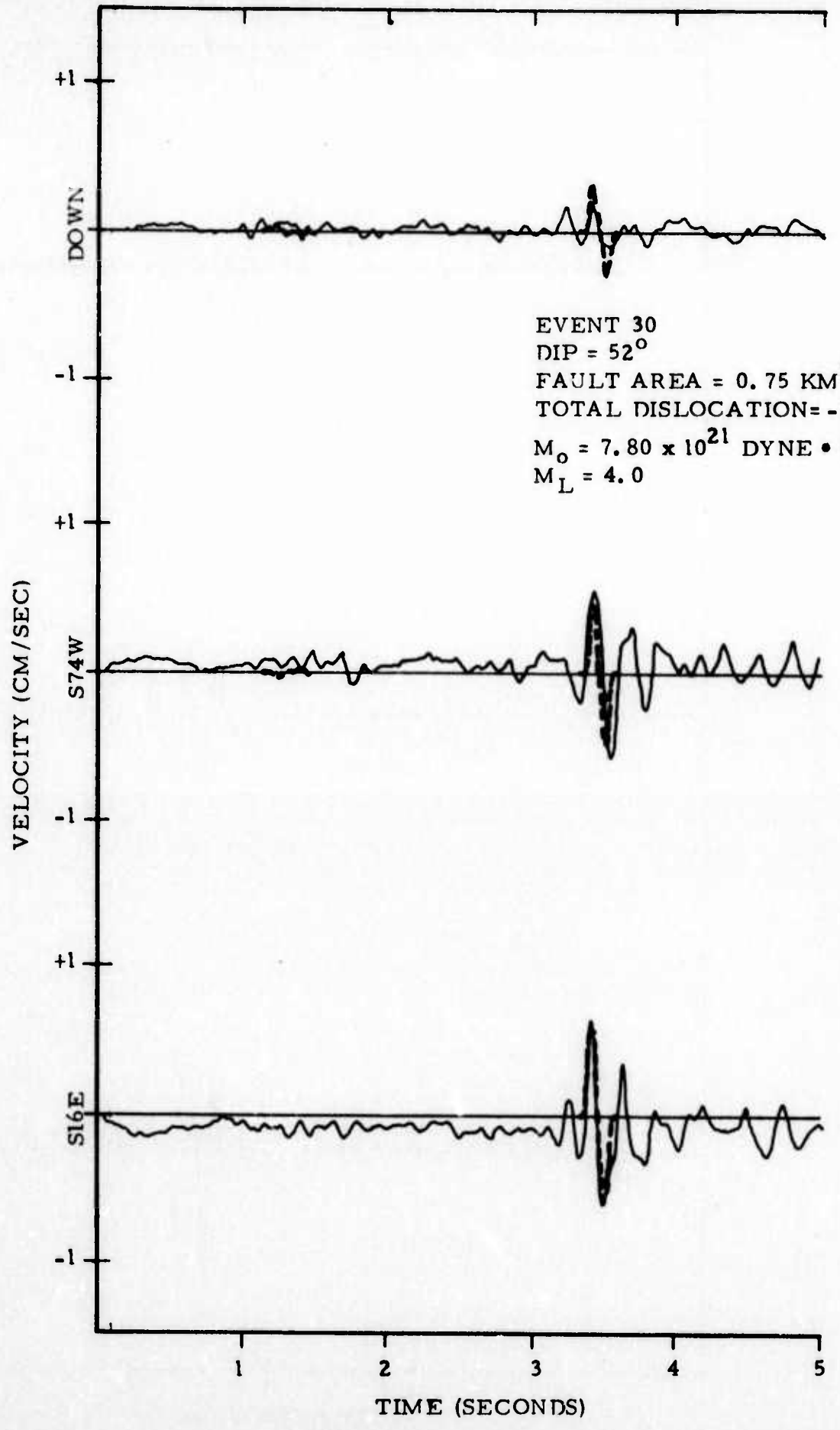

FIGURE III-7B

OBSERVED (SOLID CURVE) AND THEORETICAL (DASHED CURVE) VELOCITY WAVE OF EVENT 30 AS RECORDED AT PACOIMA DAM

TABLE III-1

SOLUTIONS TO AFTERSHOCKS USING HASKELL MOVING DISLOCATION SOURCE

PARAMETERS	EVENT 4 - ICO43	EVENT 11 - ICO44	EVENT 30 - ICO47
V_P	5.5 km/sec	5.5 km/sec	5.5 km/sec
V_S	3.2 km/sec	3.2 km/sec	3.2 km/sec
Width	1.0 km	1.0 km	0.75 km
Length	1.0 km	1.0 km	1.0 km
Rise Time	0.03 sec	0.03 sec	0.025 sec
Rupture Velocity	3.0 km/sec	3.0 km/sec	3.15 km/sec
Dip Angle	80^o	80.0^o	52^o
Azimuth	20^o	20^o	30^o
Source Coordinates X Y Z	7.84 km -5.72 km -11.0 km	5.0 km -6.35 km -8.08 km	5.0 km 7.0 km -15.0 km
Longitudinal Dislocation	-8.37 cm	-40.69 cm	-3.02 cm
Transverse Dislocation	-0.41 cm	-0.46 cm	-0.45 cm
Total Dislocation	-8.78 cm (20.0 cm)	-41.15 cm (34.0 cm)	-3.47 cm (8.0 cm)
Seismic Moment (M_o) $M_o = \mu DWL$	26.3×10^{21} dyne-cm (24.0×10^{21} dyne-cm)	123.5×10^{21} dyne-cm (67.0×10^{21} dyne-cm)	7.80×10^{21} dyne-cm (37.0×10^{21} dyne-cm)
Local Magnitude (M_L) $M_L = 0.59(\log_{10} M_o - 15.1)$	4.3 (4.9)	4.70 (5.4)	4.0 (4.6)

(Trifunac Solutions in Parenthesis)

obtained by Trifunac (1972) also given for comparison. The solutions presented here should not be considered the only correct solution, but one of the best possible within the limitations of the model.

One of these limitations is the lack of independent determination of the source parameters. Unlike the San Fernando main shock, the hypocentral location, fault dimensions, and fault orientation are relatively unknown. Also we have the usual uncertainty with rupture velocity and rise time. If we use an average rupture velocity of 3.0 km/sec (the velocity could vary between 2.3 and 4.5 km/sec [Johnson, et al. (1973)]), by varying the fault length and rise time to obtain a fit, the solution yields exceedingly short rise times.

Two approaches which could possibly help in determining a physically causal solution (with its associated rise time) are corner frequency analysis and comparison of dislocation particle velocities. First, from determination of the P-wave corner, an approximate value of V_R/L can be obtained. The corner frequency for body waves is defined to occur at the spectral transition from the low frequency trend (f^{-1}) to the high frequency trend (approximately f^{-3}) in a near-field displacement spectrum (Cherry, 1973). The corner frequency is linearly related to the ratio V_R/L, with the constant of proportionality highly variable with azimuth. Having good azimuthal coverage, and spectra where the corner is readily definable, would provide a method for determining the rise time, or at least a range of rise times. Measuring the pulse width T_1 from the velocity waveform, we can obtain the rise time from equation II-2. For the three aftershocks, this method was difficult to apply because of poor quality spectra.

The second approach involves comparison of dislocation particle velocities between the main shock and the succeeding aftershocks. The dislocation particle velocity is defined as

$$V_{DP} = \text{Dislocation/Rise Time.}$$

Because of the relatively good control on the main shock fault parameters, Tsai and Patton's value of 167 cm/sec should be fairly realistic. For the first aftershock, Tsai and Patton obtained a value of 120 cm/sec for a 0.1 second rise time. The three aftershocks yielded V_{DP} values of 282 cm/sec (event 4), 1356 cm/sec (event 11), and 121 cm/sec (event 30). Events 4 and 30 have what may be termed reasonable values compared to the main shock and the first aftershock, but event 11 seems too large. For this event, possibly a higher rupture velocity with no change in the fault length would result in a longer rise time and smaller total dislocation, thereby yielding a lower V_{DP}.

The solutions to events 4 and 11 do, in general, agree with Trifunac (1972) to the degree that they both have large dislocations over a small fault area, yielding a high stress drop. Because of the proximity of these events to the main shock, large stress concentrations seem reasonable. In the same light, event 30 has a smaller dislocation over the same fault area, and thereby a lower stress drop in concert with its relative location. Finally, events 4 and 11 have steeply dipping fault planes, indicating a stress readjustment off the main shock fault plane.

SECTION IV
SUMMARY AND FUTURE STUDIES

Our analysis of the San Fernando earthquake and three of its aftershocks recorded on strong-motion instruments at Pacoima Dam can be summarized as follows:

- Without independent estimates of the fault parameters, the credibility of the solutions obtained from the fitting procedure using the Haskell moving dislocation model is drastically reduced. Although we can use a least squares technique to fit the dislocation amplitude, the interrelationships of the fault orientation, fault dimensions, rupture velocity, and rise time make our solution highly non-unique. If strong-motion records having good azimuthal coverage and good quality accelerograms are available, reasonable estimates of fault length, rupture velocity, near-field corner frequencies, and rise time can be obtained.

- Upon generalizing our source to included segments having their own rupture velocities, dislocations, and dimensions, the effect of stick-slip alone (segmented rupture velocities) is not major within a moderate range of rupture velocities. But by having two segments with different dip angles (a hinged fault surface), significant changes do occur. In particular, the initial negative trend in the vertical S-wave trace of the main shock recorded at Pacoima Dam is produced by this fault geometry which is similar to that of the observed waveform.

- Using Jungles' and Frazier's (1973) solution, their dislocation values resulted in amplitudes much larger than the observed values when used in the Haskell model. This result is difficult to judge, considering the differences in the source mechanism descriptions and the rupture medium.

- The three aftershock solutions were characterized by small fault area (~1 km^2), moderate rupture velocities (~3 km/sec), and very short rise times (~0.03 sec). The dislocation particle velocities of events 4 and 30 correlate with those of the main shock and first aftershock, but the velocity of event 11 seems too high. Events 4 and 11, because of their large dislocations, small fault area, and proximity to the main event hypocenter, are high stress drop events, while event 30, with smaller dislocations and at a farther distance from the hypocenter, is a low stress drop event.

Future studies of near-field strong motion data will include the following:

- During a recent resurvey of the accelerometer network which recorded the San Fernando earthquake, it was determined that the horizontal components at the Pacoima Dam site were aligned incorrectly, which resulted in a 30^{o} error in the direction of the instruments. While this information was received too late for this report period, the effect of this misalignment will be determined for the next report.

- The strong motion data for the Bear Valley, California event of June 22, 1973 will be analyzed using both the Haskell whole space model and a Cagniard-de Hoop half space model refined by Johnson (1973). This approach, besides providing a detailed analysis of this event, will give an indication of the effect

that the inclusion of a half space has on our solution. Also, both near and far field spectra will be calculated to help in our parameter determination (corner frequency analysis).

SECTION V
REFERENCES

Cherry, J. T., 1973, Calculations of Near Field, Earthquake Ground Motion, Annual Technical Report, AFOSR Contract No. F44620-72-C-0051, Systems, Science and Software, La Jolla, California.

Haskell, N. A., 1969, Elastic Displacements in the Near Field of a Propagating Fault, Bull. Seism. Soc. of Amer., 59, 865-908.

Johnson, L. R., 1973, A Collection of Solutions to Lamb's Problem, Pre-Print.

Johnson, T., T. W. Francis, and C. H. Scholtz, 1973, Source Parameters for Stick-Slip and for Earthquakes, Science, 179, 278-279.

Jungles, P. H., and G. A. Frazier, 1973, Finite Element Analysis of the Residual Displacements for an Earthquake Rupture: Source Parameters for the San Fernando Earthquake, J. Geophys. Res., 78, 5062-5083.

Trifunac, M. D., 1972, Stress Estimates for the San Fernando, California Earthquake of February 9, 1971: Main Event and Thirteen Aftershocks, Bull. Seism, Soc. of Amer., 62, 721-750.

Tsai, Y. B., and H. J. Patton, 1972, Near-Field Small Earthquakes - Dislocation Motion, Semi-Annual Technical Report No. 1, AFOSR Contract No. F44620-72-C-0073, Texas Instruments Incorporated, Dallas, Texas.

Tsai, Y. B., and H. J. Patton, 1972, Dislocation Motion and Theoretical Far-Field Source Spectra of Four California Earthquakes, Semi-Annual

Technical Report No. 2, AFOSR Contract No. F44620-72-C-0073, Texas Instruments Incorporated, Dallas, Texas.

Whitcomb, J. H., C. R. Allen, J. D. Garmany, and J. A. Hileman, 1973, San Fernando Earthquake Series, 1971: Focal Mechanisms and Tectonics, Rev. of Geophys. and Space Phys., 11, 693-730.